

Carbon Dioxide-Induced Plasticization of Polyimide Membranes: Pseudo-Equilibrium Relationships of Diffusion, Sorption, and Swelling

John D. Wind,[†] Stephen M. Sirard,[†] Donald R. Paul,[†] Peter F. Green,[†] Keith P. Johnston,[†] and William J. Koros^{*,‡}

Department of Chemical Engineering, The University of Texas at Austin, Texas 78712, and School of Chemical Engineering, Georgia Institute of Technology, Atlanta, Georgia 30332

Received March 20, 2003; Revised Manuscript Received May 29, 2003

ABSTRACT: The application of membranes in gas separation and pervaporation requires materials that are resistant to plasticizing feed streams. We demonstrate the relationship between CO₂ sorption, permeability, and film swelling of a polyimide gas separation membrane and how these properties are affected by systematic changes to the polymer structure induced by thermal annealing and covalent cross-linking. Dilation of polyimide thin films (~120 nm) exposed to high-pressure CO₂ (up to 100 atm at 35 °C) was measured by in situ spectroscopic ellipsometry to decouple the effects of thermal and chemical treatments on the film swelling. The refractive index of the CO₂-swollen polymer is also used to estimate the CO₂ sorption for comparison against that measured on thick films (~50 μm) by the pressure-decay method. Differences in sorption levels in thin and thick films appear to be related to accelerated physical aging of the thin films. Both thermal annealing and covalent cross-linking of the polyimide films reduce polymer swelling to prevent large increases in the CO₂ diffusion coefficient at high feed pressures. The CO₂ permeability and polymer free volume strongly depend on the annealing temperature, and different effects are observed for the cross-linked and un-cross-linked membranes. The so-called "plasticization pressure" in permeation experiments (i.e., upturn in the permeation isotherm) appears to correlate with a sorbed CO₂ partial molar volume of 29 ± 2 cm³/mol in the polymer. Furthermore, cross-linking of high glass transition polyimides produces a much greater reduction of the CO₂-induced dilation than does cross-linking of rubbery polymers such as PDMS for swelling up to 25%.

Introduction

Compressed CO₂ is an attractive alternative solvent because it is nontoxic, nonflammable, and inexpensive and has easily tunable solvent properties near the critical point. Carbon dioxide is a very effective processing aid for swelling^{1–4} and plasticizing polymers^{5–8} to promote the impregnation, extraction, and foaming of polymer films.^{9,10} Despite these positive aspects, the high pressures required in supercritical applications and the expensive nature of most CO₂ surfactants and stabilizers make the development of processes for high-pressure separations of CO₂ from small molecules important to control operating costs. Polymeric membranes have potential for these types of separations.¹¹ However, CO₂-induced swelling and plasticization are detrimental to membrane performance. Thus, designing high-performance membranes for such applications is a difficult challenge that requires a better understanding of the interactions between polymers and high-pressure CO₂.

Polyimide membranes have excellent gas separation properties for applications where the preferentially permeated species has a larger diffusion coefficient than other components in the feed mixture. Removal of CO₂ from natural gas streams exemplifies this type of separation. However, the process would be more attractive if membranes can be developed that are better able to maintain high selectivity in the presence of condensable plasticizing components such as CO₂.

It is desirable to work with soluble polyimides that can be easily cast into films or spun into asymmetric hollow fibers. Polyimides synthesized from (4,4'-hexafluoroisopropylidene)diphthalic anhydride (6FDA) tend to have excellent transport properties and solution processing characteristics but are susceptible to plasticization. The two most common approaches for stabilizing these materials have been cross-linking^{12–14} and/or thermal treatments.^{15,16} To establish a stability criterion, it is necessary to decouple the physical annealing and chemical cross-linking that occur simultaneously during the thermal treatment.

The effect of cross-linking on the sorption and dilation of CO₂ in rubbery polymers may be estimated through the Flory model. On the other hand, the physical phenomena associated with swelling of cross-linked glassy polymers are quite different, so this model is inadequate. Comparisons have been made regarding the partial molar volume of CO₂ in rubbery and glassy polymers,^{1,4,17} but it is not clear how the partial molar volume is affected by the structure of the glassy polymer. In this paper we probe the effect of polymer chain rigidity on the sorbed CO₂ partial molar volume to understand how the polymer properties are affected by the sorbed CO₂ and the implications this has for membrane separations.

The use of in-situ spectroscopic ellipsometry is a powerful tool for analyzing thin film sorption and dilation. These measurements are important because the separating layers on industrial asymmetric hollow fiber membranes are very thin (~0.1 μm), and thin films can sorb differently¹⁸ and plasticize at lower pressures¹⁹ than thick films of the same material. Thin films may

[†] The University of Texas at Austin.

[‡] Georgia Institute of Technology.

* Corresponding author: Tel +1-404-385-2684; Fax +1-404-385-2683; e-mail wjk@che.gatech.edu.

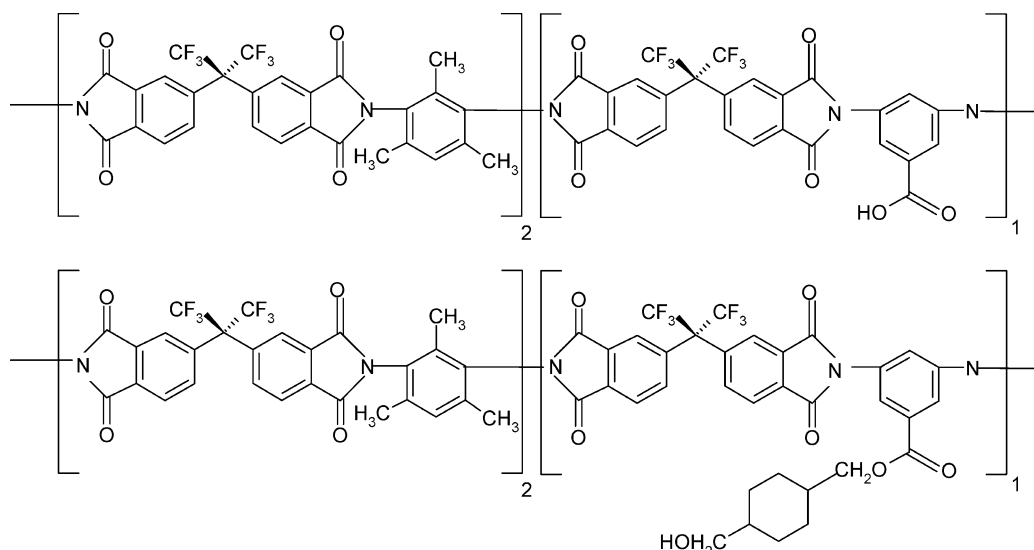


Figure 1. Polymer structures (6FDA-DAM:DABA 2:1): free acid and cyclohexanedimethanol (CHDM) monoester.

also behave differently because of reduced packing density of the polymer segments at the free surface due to an increased configurational entropy.^{20,21} Thus, spectroscopic ellipsometry enables characterization of the dilation and sorption of thin polymer films where more traditional “bulk techniques” (e.g., dilatometry for dilation and pressure-decay for sorption) are not applicable.

Complications in the analysis of sorption in glassy polymers by simple interferometric techniques arise from the difficulty of independently decoupling the thickness and refractive index from the optical data.²² In contrast, multiwavelength spectroscopic ellipsometry can independently determine the thickness and refractive index of a thin film, allowing for reasonably accurate estimates of sorption levels in rigid glassy polymers. In addition, a CO₂-induced T_g (or P_g) may also be determined from the hysteresis behavior of the sorption and desorption curves.²³

An understanding of how a membrane's structure affects its susceptibility to CO₂-induced plasticization is needed in order to effectively design polymeric membranes for high-pressure CO₂ separations. The main objective of this work is to understand how the sorption, dilation, and diffusion processes are coupled in a plasticized gas separation membrane and how the polymer structure may be modified by thermal annealing and chemical cross-linking to control the diffusion coefficient in the presence of high CO₂ concentrations. Spectroscopic ellipsometry was used to measure the dilation and estimate the CO₂ sorption in high- T_g (~360 °C) polyimide thin films with various heat treatments and chemical cross-linking. Sorption measurements on relatively thick (~50 μm) free-standing films by the pressure-decay method are compared with the ellipsometric measurements for the supported thin films. The sorption and dilation data are used to calculate the CO₂ partial molar volume in the polymer. Plasticization of the polymer in permeation experiments is shown to correlate with changes in the sorbed CO₂ partial molar volume. This correlation is then used to suggest why these polyimides plasticize and why covalent cross-linking and heat treatment are effective approaches for stabilizing these membranes. Relaxation-controlled aspects of these phenomena are explored in a separate publication.²⁴

Experimental Section

Polymer Synthesis. Figure 1 shows the structures of the 6FDA-DAM:DABA 2:1 polyimide, untreated and monoesterified with 1,4-cyclohexanedimethanol (CHDM). The polycondensation was performed by the reaction of 6FDA with diaminomesitylene (DAM) and 3,5-diaminobenzoic acid (DABA) in NMP, followed by a chemical imidization with an equimolar mixture of triethylamine and acetic anhydride, described in detail elsewhere.²⁵ All reagents were obtained from Sigma-Aldrich, except for 6FDA, which was obtained from Lancaster.

The DABA moiety provides a carboxylic acid group which can be esterified with glycol compounds to form cross-linked polymers.^{13,14} The monoesterification reaction was carried out at 140 °C for 16 h in NMP. The reaction flask was fitted with a condenser and a continuous nitrogen purge. After completion of the monoesterification reaction, the polymer solution was cooled to room temperature, and the polymer was precipitated in methanol, blended, filtered, and washed with methanol. The monoesterification yield was 50%, as measured by NMR spectroscopy.²⁶ It was then dried at 70 °C for 24 h under vacuum. The films for permeation and sorption were cast on Teflon surfaces from 3 wt % solutions in THF in a glovebag to promote slow evaporation of the solvent. The polymer films were dried under vacuum for 24 h at various temperatures to activate the solid-state transesterification cross-linking reaction.

Steady-state gas permeabilities were determined at 35 °C with a constant volume, variable pressure apparatus.²⁷ The membrane area was measured with Scion Image software, and the film thickness was measured with a micrometer (Ames). Permeation measurements for feed pressures above 10 atm were made every 24 h to capture the slow relaxations involved in plasticization. Previously, it was shown how plasticization, as measured by changes in the diffusion or permeation coefficient, is a function of time and CO₂ feed pressure.^{5,14} The CO₂ solubility in bulk polymer films was measured in a pressure-decay sorption apparatus.²⁸ Dilation measurements of supported thin film samples were performed with high-pressure in situ spectroscopic ellipsometry.¹⁸

Sample Preparation for Supported Thin Films. Silicon (100) wafers (Wafer World) were cut into 1 cm × 1 cm squares. The wafers were cleaned²⁹ by initially soaking in a 50/50 (w/w) hydrochloric acid (EM Science)/methanol (EM Science) solution for 30 min. The wafers were then rinsed with excess deionized water (NANOpure II, Barnstead) and dried with nitrogen gas (Matheson Gas Products, >99.999%). The wafers were then soaked in 95% sulfuric acid (Mallinckrodt) for 30 min and subsequently rinsed with deionized water and dried with nitrogen gas. The native oxide thickness was measured for each wafer with spectroscopic ellipsometry prior to coating

Table 1. Polyimide Solubility for Various Thermal and Chemical Treatments

polymer	esterification	thermal treatment (°C)	solubility in NMP at 120 °C after 5 days
6FDA-DAM	none	295	soluble
6FDA-DAM:DABA 2:1	none	220	soluble
6FDA-DAM:DABA 2:1	none	295	gelled
6FDA-DAM:DABA 2:1	CHDM	220	gelled

with polymer. The native oxide was between 1.5 and 2.0 nm thick for all of the samples.

To prepare the supported thin films, the polyimide was initially dissolved in 2-methyl-4-pentanone (Aldrich, 99+%). The solution was then spin-coated onto the silicon wafers by using a photoresist spinner (Headway Research, Inc.). The concentration of the solution was adjusted in order to achieve films of the desired thickness at a spin rate of 3000 rpm. The thin films were heat treated under vacuum at their respective temperatures for 24 h.

Ellipsometry. A M-44 spectroscopic ellipsometer (J.A. Woollam, Co., Inc.), set up in the rotating analyzer configuration, was used for all of the experiments. The angle of incidence for all measurements was 70° from the vertical. The experiments were performed in a specially designed high-pressure ellipsometry cell. The details of the cell design can be found elsewhere.^{18,23} The wavelength range for the experiments is 410–750 nm. Detailed descriptions of the theoretical aspects of ellipsometry can be found elsewhere.^{30,31}

After loading the samples in the high-pressure cell, CO₂ (Air Products, >99.9999%) was charged to the cell using a manual pressure generator (High-Pressure Equipment Co.). Pressure was controlled with a strain gauge pressure transducer (Sensotec). The cell was heated using four cartridge heaters (Omega) that were inserted in the top of the cell. The cell was allowed to reach thermal equilibrium for 30 min before scans were taken. Measurements were made approximately every 15 min between pressure increments. The nominal Fickian equilibration times were less than 30 s, so the films were in a relaxation-controlled state when the dilation measurements were made.

The thickness and refractive index of the swollen films were extracted from the ellipsometry data by assuming a four-layer optical model. The model consists of a CO₂ atmosphere, a swollen polymer layer, a SiO₂ native oxide, and a silicon substrate. Literature values were used for the refractive index of the CO₂ atmosphere,³² the SiO₂ native oxide,³³ and the silicon substrate.³⁴ The fitting parameters for the swelling experiments were the thickness and refractive index of the swollen polymer film and the offset in the ellipsometric angle, Δ , due to window birefringence. The refractive index of the swollen polymer film was modeled using a Cauchy dispersion relationship,³¹ $n(\lambda) = A + B/\lambda^2 + \dots$

Results

Polymer Film Solubility. Thermal treatments of polyimide films can significantly change their solubility properties.³⁵ Table 1 shows how the solubility of the polymers in NMP at 120 °C changed with annealing temperature. When annealed at 220 °C, the 6FDA-DAM:DABA 2:1 film is completely soluble in NMP. In contrast, when annealed at 295 °C, the 6FDA-DAM:DABA 2:1 film becomes insoluble and more amber colored. To investigate this peculiar change in solubility with increased annealing temperature, a 6FDA-DAM film was also annealed at 295 °C. After annealing, the 6FDA-DAM film remained completely soluble and colorless. Therefore, it appears that the changes in solubility are associated with the presence of the DABA moiety. IR spectra of the 2:1 with free acid groups did not show any differences with respect to annealing temperature, suggesting that there is no chemical reaction occurring

without deliberate esterification.³⁶ Changes in film color with annealing are typically attributed to the formation of charge-transfer complexes (CTC), between the electron-donating diamine moieties and the electron-accepting imide moieties.³⁷

Permeation and Sorption Isotherms for Bulk Free-Standing Films. The permeability (P_A) of a gas molecule “A” through a dense polymeric membrane is defined as the flux (n_A), normalized by the transmembrane partial pressure (Δp_A) and membrane thickness (l),

$$P_A = n_A \frac{l}{\Delta p_A} \quad (1)$$

Permeability values are typically reported in Barrers [1 Barrer = 10⁻¹⁰ cm³ (STP) cm/(cm² cmHg s)].

According to the well-known solution-diffusion mechanism, the permeability can be written as the product of the diffusion coefficient, D_A , and the solubility coefficient, S_A

$$P_A = D_A S_A \quad (2)$$

The solubility coefficient, S_A , is related to the condensability of the penetrant, the polymer–penetrant interactions, and the free volume in the glassy polymer. The average diffusion coefficient, D_A , is a measure of the mobility of the penetrant between the feed and permeate faces of the membrane. It depends on the packing and motion of the polymer segments and on the size and shape of the penetrating molecules.

Similar in form to the Doolittle equation that describes the fluidity of simple hydrocarbon liquids,³⁸ Cohen and Turnbull developed an expression for the diffusion coefficient of hard spheres in a glass³⁹

$$D = A \exp\left(\frac{-\gamma v^*}{v_f}\right) \quad (3)$$

where A and γ are constants, v^* is the critical volume of gap opening to allow a diffusive jump, and v_f is the average free volume per sorbed molecule in the glass. In this paper, it is shown how the CO₂ partial molar volume is affected by plasticization and how the CO₂ diffusion coefficient increases as a result, consistent with eq 3.

Heat treatment of aromatic polyimides is an effective approach for reducing CO₂ plasticization in high-pressure membrane separations. Polyimides tend to become more colored with thermal treatments, presumably showing the formation of charge-transfer complexes and physical aging.¹⁶ Figure 2 shows the effect of annealing temperature and covalent cross-linking of the 6FDA-DAM:DABA 2:1 polyimide on the CO₂ permeation isotherms. The “plasticization pressure” may be defined as the pressure at which there is a minimum in the isotherm. High-temperature thermal treatments generally increase the plasticization pressure for both the films with free acid groups and those that are cross-linked, but covalent cross-linking offers somewhat better plasticization resistance than a simple heat treatment at 220 °C and much better resistance to organic solvents. Cross-linking the 2:1 polymer with 1,4-butanediol offers even better resistance to CO₂ plasticization.²⁶

The solubility coefficient, S_A , for gas sorption in glassy polymers is often described by the dual mode model⁴⁰

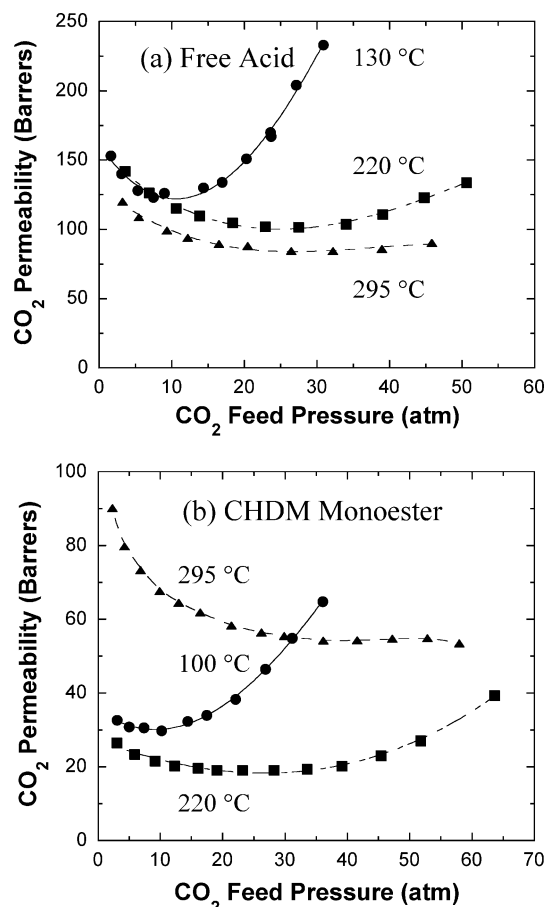


Figure 2. CO₂ permeation isotherms at 35 °C for 2:1 bulk films with various thermal and cross-linking treatments: (a) free acid annealed at 130, 220, and 295 °C; (b) CHDM monoester cross-linked at 100, 220, and 295 °C.

$$S_A = \frac{C_A}{p_A} = k_{DA} + \frac{C_{HA}b_A}{1 + b_A p_A} \quad (4)$$

where C_A is the concentration, p_A is the partial pressure, k_{DA} is the Henry's law constant, C_{HA} is the Langmuir capacity constant, and b_A is the Langmuir affinity constant. The CO₂ sorption isotherms in Figure 3 show that thermal annealing of the 6FDA-DAM:DABA 2:1 films with free carboxylic acid groups tends to decrease the CO₂ sorption, especially at high pressures. Surprisingly, the sorption curves for the 220 and 295 °C treatments are not too different, despite the fact that the solubility of these films in organic solvents (THF, NMP, etc.) is very different (Table 1).

The dual mode sorption parameters for CO₂ are shown in Table 2. For the films with free acid groups, higher temperature thermal annealing decreases the Langmuir capacity constant, $C_{H'}$, which is consistent with an accelerated physical aging process, where the free volume decreases by a diffusive mechanism.⁴¹ The Henry's law sorption coefficient, k_D , is also reduced significantly with higher temperature annealing, reflecting the lower sorption at high pressures, where plasticization effects are observed.

The CHDM monoesters (i.e., cross-linkable polymer with pendant cyclohexanedimethanol groups) show different sorption behavior with respect to the annealing temperature. Similar to the untreated polymer, the Henry's law sorption coefficient, k_D , is also significantly reduced with heat treatment, but it has a greater

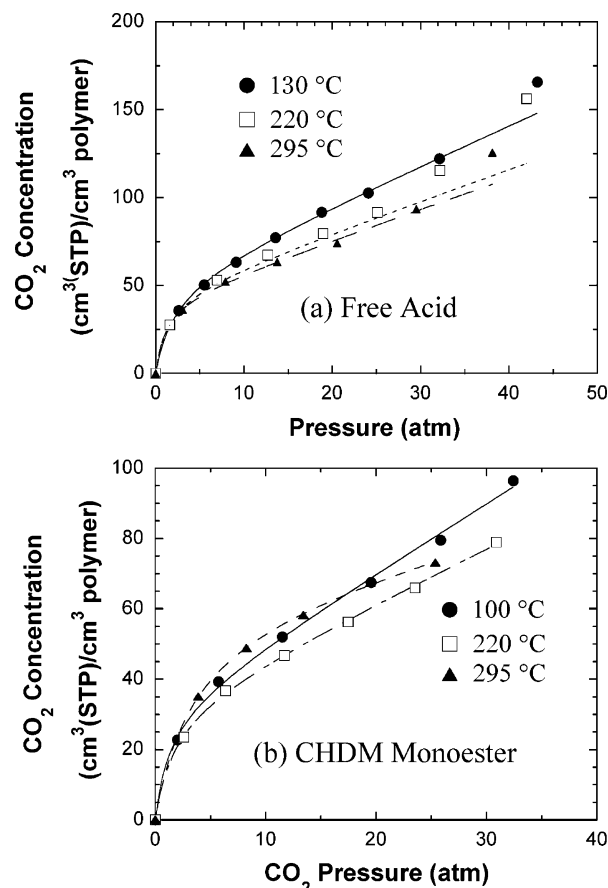


Figure 3. CO₂ sorption isotherms at 35 °C for 2:1 bulk films with various thermal and cross-linking treatments: (a) free acid annealed at 130, 220, and 295 °C; (b) CHDM monoester cross-linked at 100, 220, and 295 °C. The curves represent the dual mode model fits for pressures below 25 atm.

Table 2. CO₂ Dual Mode Sorption Parameters from Ellipsometry and Pressure-Decay Measurements^a

thermal treatment	ellipsometry		pressure-decay		<i>b</i>
	k_D	$C_{H'}$	k_D	$C_{H'}$	
130 °C free acid	2.06	15.9	2.23	54.2	0.454
220 °C free acid	1.80	20.0	1.77	46.6	0.689
295 °C free acid	1.13	21.0	1.74	42.4	0.896
100 °C CHDM	1.73	14.4	1.82	31.1	0.51
220 °C CHDM	1.49	10.5	1.36	37.0	0.58
295 °C CHDM	1.02	25.1	0.814	59.9	0.29

^a k_D (cm³ (STP)/(cm³ polymer atm)), $C_{H'}$ (cm³ (STP)/(cm³ polymer)), and b (1/atm).

temperature dependence than is seen for the films with free acid groups. On the other hand, the Langmuir capacity constant, $C_{H'}$, increases with increased annealing temperatures for the CHDM monoester samples, indicating an increase in *unrelaxed* free volume within the films with cross-linking.

Dilation of Supported Thin Films. The dilation of glassy polymers is complicated by the different sorption mechanisms of hole-filling and dissolution. Various theoretical studies have been reported^{42,43} along with experimental characterization by dilatometry⁴⁴ and optical interferometry.^{2,22} Optical interferometry gives the product of the film thickness and the refractive index, thus requiring a known relationship between refractive index and thickness. Ellipsometry offers the advantage in that thickness and refractive index are determined independently.^{30,31}

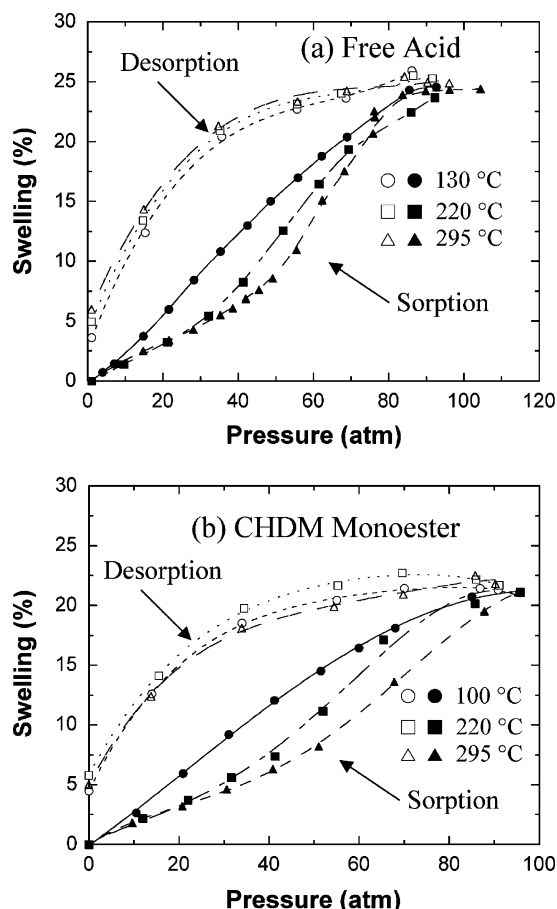


Figure 4. CO₂ dilation isotherms at 35 °C for 2:1 thin films with various thermal and cross-linking treatments: (a) free acid annealed at 130, 220, and 295 °C; (b) CHDM monoester cross-linked at 100, 220, and 295 °C.

The dilation and consolidation isotherms are shown in Figure 4. It is clear that increasing the annealing temperature leads to lower dilation at pressures below 80 atm, but above this pressure the swelling is very similar for all three films, for a given polymer composition. For the desorption isotherms, large hysteresis is observed, reflecting the slow chain relaxations that are characteristic of glassy polymers. All of the polyimides studied here have T_g s of approximately 360 °C. Hysteresis in the sorption/desorption curves indicates that the CO₂ has not induced a glass transition up to 80 atm, contrary to the results observed for PMMA,²³ even though the CO₂ sorption is roughly twice as high as that of PMMA. Therefore, other techniques such as creep compliance⁴⁵ should be utilized to determine the in situ T_g .

In the study of high-pressure CO₂ sorption and dilation in PMMA, several researchers have assumed that an inflection point (i.e., upturn) in the swelling isotherm corresponded to the isothermal glass transition.^{3,4} However, it is clear from Figure 4 that for an unconditioned polymer there can be an inflection in the swelling isotherm without a glass transition. Interestingly, for the un-cross-linked films treated at 130 and 220 °C, the pressures at which the inflection occurs (and the isotherms diverge from each other), 12 and 30 atm, respectively, correspond to the respective plasticization pressures in the permeation isotherms (Figure 2). Similar results are seen for the CHDM monoester films. At 90 atm, the three thermally annealed un-cross-linked samples all have similar swelling, indicating that CO₂

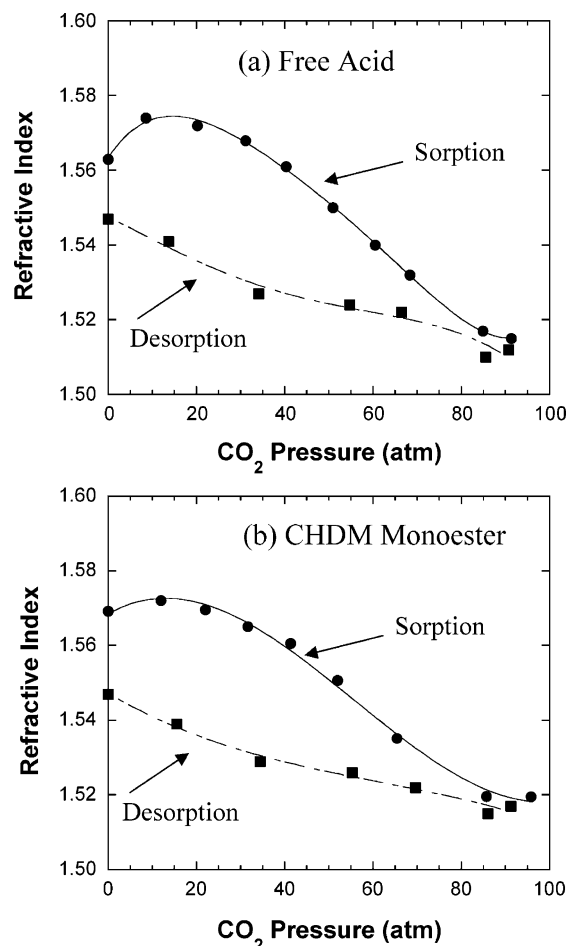


Figure 5. Refractive index of CO₂-swollen polymers at 35 °C (both films annealed at 220 °C): (a) free acid; (b) CHDM cross-linked.

may disrupt the physical interactions (e.g., charge-transfer complexes) promoted by thermal annealing. CO₂ can act as a Lewis acid and have favorable interactions with the polar polyimide.⁴⁶ The desorption isotherms for these samples are also quite similar, though the higher the treatment temperature, the greater the hysteresis.

Estimation of CO₂ Sorption from Refractive Index for Supported Thin Films. The solubility of gases in polymers can be measured by the pressure-decay method or by gravimetric means. The sorption can also be estimated from the refractive index of the solvent-laden polymer. A major advantage of using spectroscopic ellipsometry is that both dilation and sorption can be estimated simultaneously.

The refractive index isotherms of an un-cross-linked and a cross-linked film annealed at 220 °C are shown in Figure 5. For both films, as the pressure is increased the refractive index initially increases as the microvoids are filled with CO₂ and the polymer plus sorbed CO₂ shows a higher density. Once these voids are saturated, the refractive index decreases with increasing CO₂ pressure as the polymer becomes less dense with the increased sorption of CO₂ into the polyimide. The sharp drop in the index around 75 atm likely arises in part to excess CO₂ sorbed onto/into the polymer due to compressibility effects, as was observed for PMMA.²³ At 35 °C, this critical sorption of CO₂ should only occur over a small pressure range. After exposure to high-pressure CO₂ (100 atm), the film contracts as the CO₂ pressure

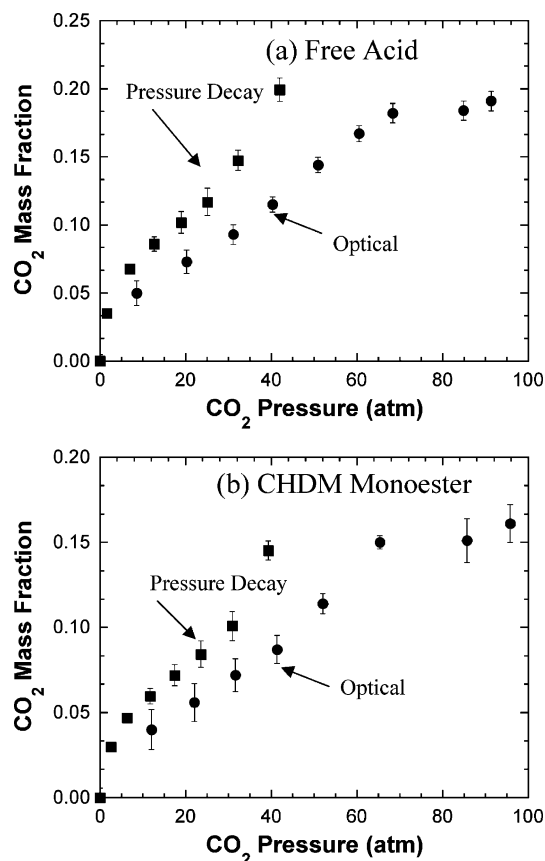


Figure 6. CO₂ sorption at 35 °C by refractive index and pressure-decay techniques for films annealed at 220 °C: (a) free acid; (b) CHDM cross-linked.

is decreased but does not reach its preconditioned state. The result of this partial relaxation of the polymer chains (i.e., excess free volume) is a lower refractive index, as shown in Figure 5.

The procedure for estimating sorbed CO₂ mass fractions from the Clausius–Mosotti equation has been described previously.^{18,47} The CO₂ density and refractive index in the polymer were assumed to be 1.0 g/cm³ and 1.233, respectively.⁴⁸ Since the CO₂ densities and refractive index are linearly correlated,⁴⁸ the values chosen do not have a significant effect on the calculated concentration by the Clausius–Mosotti method. Figure 6 shows a comparison of the ellipsometric and pressure-decay sorption measurements for the 2:1 films treated at 220 °C, with and without cross-linking.

The sorption via Henry's law mechanism (characterized by k_D) agrees reasonably well between the pressure-decay and ellipsometric techniques as seen in Table 2. The offset in total sorption shown in Figure 6 for both films primarily reflects differences in the Langmuir sorption capacity. The amount of unrelaxed free volume in a glassy polymer is dependent on the polymer structure and the thermal history. Aging effects in glassy polymers are more significant in thin films, as it is envisioned that the film densifies by a mechanism of diffusion of free volume to the free surface of the film. The characteristic path length for this diffusion determines the amount of aging at a given time.⁴¹ The films used for the ellipsometry experiments were approximately 120 nm thick, whereas the films used for the pressure-decay sorption were approximately 50 000 nm thick. The characteristic aging time scales as the film thickness squared, so there will be significant differ-

ences in the aging of the two films via this aging mechanism. Thus, lower C_H s for the thin films relative to the thicker bulk films are expected. Table 2 shows the dual mode sorption parameters for the pressure-decay and optical sorption measurements. The thin films have significantly lower C_H s than the thick films. In general, both techniques give consistent trends regarding the effect of heat treatment and chemical cross-linking on the sorption of CO₂ in the membranes. The Langmuir affinity constants (b) were not fit for the ellipsometry data because of insufficient data points in the low-pressure region. They were assumed to be the same as those for the bulk films.

Discussion

CO₂-induced plasticization in polyimide membranes can be reduced through simple thermal annealing.¹⁶ Both the physical and the chemical properties of polyimides can be altered with heat treatments as shown by the change in the solubility of the polyimide films in NMP. There are several factors that could contribute to this change in solubility. From Table 1, it appears that the changes in solubility are associated with the presence of the DABA moiety. The COOH groups may dimerize to form physical cross-links. Furthermore, it is known that polyimide solubility is related to the electron delocalization, which is affected by the packing density (steric effects) and the presence of electron-withdrawing groups.⁴⁹ Typically in the solid-state, intermolecular charge-transfer complexes (CTC) dominate over intramolecular CTC via π -bonding overlap between donor and acceptor moieties.⁵⁰ Since the torsional angle of the nitrogen–phenyl bond is an important parameter in controlling the formation of charge-transfer complexes,³⁷ the meta-connected DABA without the bulky methyl groups on the aromatic ring may be sterically more favorable for overlapping the diamine moieties (electron donors) with the dianhydride moieties (electron acceptors). However, electron-withdrawing groups on the diamine moiety (i.e., COOH) usually disrupt charge-transfer complexes. It is likely the heat treatment at 295 °C makes the normally soluble 2:1 polyimide insoluble due to a combination of the aforementioned effects. In addition, the lower CO₂ sorption at high pressures for the films annealed at higher temperatures is also likely due to these changes to the polymer chain interactions.

Increasing the annealing temperature also results in better resistance to plasticization in the permeation isotherms for both the un-cross-linked and the cross-linked films. Since the permeation is directly related to the solubility of CO₂ in the films, it is useful to examine the effects of annealing temperature and chemical cross-linking on the CO₂ sorption isotherms. As seen in Table 2 and Figure 3, the CO₂ sorption for the un-cross-linked polyimides decreases with increasing annealing temperature. This appears to occur in part due to faster physical aging with increasing annealing temperature, where free volume is believed to diffuse out of the film. This increased aging is consistent with the decreases in C_H' with annealing temperature.

Cross-linking with CHDM appears to markedly change the contribution of the sorption from hole filling and matrix dilation modes relative to the situation for the polymers with free acid groups. While both the cross-linked and the un-cross-linked films show similar trends in terms of how k_D is affected by annealing temperature,

the cross-linked films show an increase in C_H' with increased annealing temperature. An increase in C_H' suggests that the unrelaxed free volume in the polymer is increasing, resulting in a larger contribution of "hole filling" to the total CO₂ sorption. This is consistent with the permeation results in Figure 2, where the annealing at 295 °C increases the permeability (due to increased free volume) with greater "dual mode" behavior, reflected by sharper decreases in permeability with increasing feed pressures (below 10 atm). This increase in free volume may arise from the insertion of cross-linking segments between the polymer chains that ultimately disrupt the chain packing. Free volume may also be created by the concomitant elimination of the large, bulky pendant CHDM groups that occurs during the transesterification cross-linking reaction.

Overall, the effects of annealing temperature and chemical cross-linking on the CO₂ sorption are small compared to the large effects seen in the permeation isotherms. Equation 2, therefore, suggests that the large changes in the permeation isotherms result from the effects that thermal annealing and chemical cross-linking have on the penetrant *diffusion coefficient*. Thus, both covalent cross-linking and higher thermal annealing temperatures stabilize the CO₂ diffusion coefficient in the membrane, even when exposed to high-pressure CO₂. The effects on the diffusion coefficient appear to be related to the dilation of the polymer. As seen in Figure 4, the dilation is reduced with increased annealing temperatures for both the un-cross-linked and the cross-linked films, and the pressures at which the dilation isotherms diverge correlate to the plasticization pressures in Figure 2. For the cross-linked films, increased annealing temperatures help drive the cross-linking reaction, which causes the polymer chain mobility to be more restricted. Restricting the chains causes the films to be more resistant to dilation, thus controlling the diffusion coefficient and providing stronger resistance to CO₂-induced plasticization.

We speculate that the local chain segmental mobility near a diffusing penetrant should be reflected by the penetrant partial molar volume in the polymer, since this is related to the amount of free volume added to the polymer by sorption of the penetrant. For the unidirectionally dilating film attached to the silicon substrate, the partial molar volume of CO₂ in the polymer can be calculated by⁵¹

$$v_{\text{CO}_2} = 22400 \left[\frac{\partial(h/h_0)}{\partial C} \right]_{T,p} \quad (5)$$

The partial molar volumes are shown in Figure 7 for the films with free acid groups and the CHDM monoester annealed at various temperatures. These values were calculated from the ellipsometry data. As the pressure increases the partial molar volumes increase, reflecting the saturation of the Langmuir sites (since preexisting holes do not require as much dilation) and plasticization of the polymer.

The diffusion coefficient of a penetrant in a dense polymeric membrane is envisioned to occur by molecules jumping through transient free volume openings arising from thermal fluctuations of the polymer chains. This dynamic free volume distribution is affected by the sorption of plasticizing components in a complex manner. The diffusion coefficient is dependent on a mol-

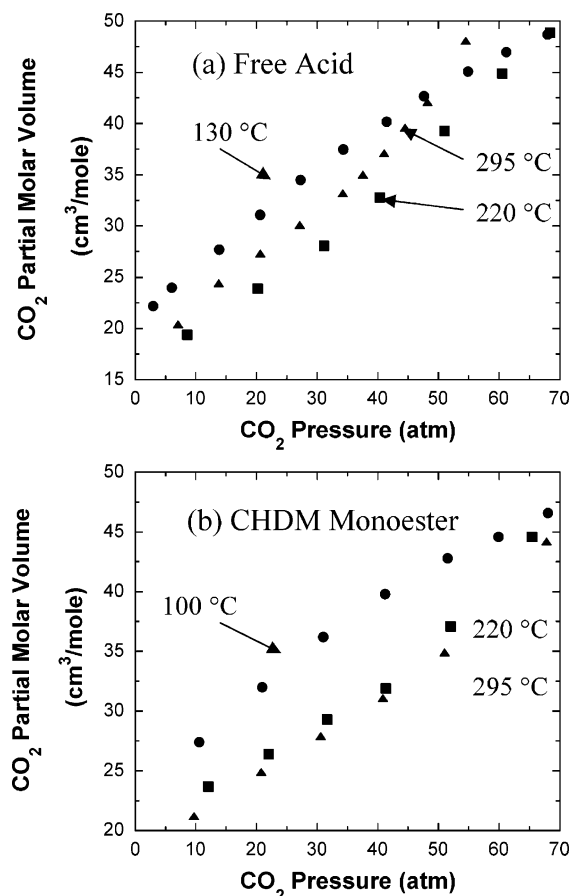


Figure 7. CO₂ partial molar volume at 35 °C from ellipsometry data: (a) free acid; (b) CHDM cross-linked.

Table 3. Plasticization Pressure, Concentration,^a and Swelling for Various Membranes at the Onset of Permeation Plasticization

thermal treatment	plasticization press. (atm)	concn (cm ³ (STP)/ (cm ³ polymer)	CO ₂ partial molar volume (cm ³ /mol)
130°C free acid	12	38	27
220°C free acid	30	73	28
100°C CHDM	12	33	28
220°C CHDM	36	64	31

^a At upstream face of membrane, based on optical sorption measurements.

ecule's size relative to the size and frequency of the transient gaps in the polymer matrix. Figure 7 shows that higher temperature annealing generally leads to lower CO₂ partial molar volumes at a given pressure.

The dilation isotherms in Figure 4 show upward inflections at higher pressures, depending on the specific chemical or thermal treatment. The pressures at which the dilation curves diverge from each other (for increasing pressures) correspond to the plasticization pressures in permeation experiments (see Figure 2). It has been suggested by other researchers that a critical CO₂ concentration of 37 ± 7 cm³ (STP)/cm³ is required for plasticization of a series of glassy polymers in permeation tests at 25 °C.⁷ However, we find that the plasticization pressure is not well correlated with the CO₂ concentration. Table 3 shows the CO₂ concentration and partial molar volume at the plasticization pressure for the membranes that have significant plasticization. These data suggest that the onset of plasticization may be more closely related to a threshold value of the sorbed

CO₂ partial molar volume of $\sim 29 \pm 2$ cm³/mol. The partial molar volume of CO₂ in various organic liquids is ~ 46 cm³/mol.¹ If plasticization is seen as a precursor to a solvent-induced glass transition at the measurement temperature, one might envision that reaching this critical partial molar volume allows for a specific magnitude of local segmental motion. Such motion, although insufficient for true rubberlike large-scale rotational motion, may be adequate to allow for dramatically higher CO₂ diffusion rates compared to the rigid, neat glassy matrix. For diffusion in rubbery polymers, Struk developed a model in which the diffusion coefficient is related to the partial molar volume,⁵² and this is consistent with our results for plasticized glassy polymers. Additionally, Bohning and Springer showed that the sorbed CO₂ partial molar volume is significantly increased by slow polymer relaxations when its value exceeds 30 cm³/mol in polysulfone and poly(ether sulfone).⁵³

We hypothesize that the excessive mobility facilitated by the sorbed CO₂ in the normally well-packed regions (Henry's law) causes an increase in the CO₂ diffusion coefficient. In calculating the CO₂ partial molar volume, it is assumed that all of the dilated volume is occupied by CO₂. In reality, it is likely that some of this dilation is caused by the increased polymer segmental mobility (vibrational and rotational). Therefore, it seems quite reasonable that the plasticization pressure should correlate with some threshold of the sorbed penetrant partial molar volume since this parameter incorporates the excess polymer occupied volume due to the increased mobility. This is consistent with the observations of Sanders where plasticization in a series of polymers was correlated with the mobility of side groups on the polymer chain and not main-chain parameters such as the glass transition.⁸

For these rigid polyimides, restricted mobility due to cross-linking suppresses increases in segmental mobility facilitated by the sorbed CO₂. These effects are similar to those seen in ionomers, where the rigidifying effects of ionic clusters increases as the rigidity of the matrix polymer increases.⁵⁴ For rubbery polymers such as poly(dimethylsiloxane), the effect of cross-linking on CO₂ swelling can be modeled with the Flory expression⁵⁵

$$\ln a = \ln \Phi_2 + (1 - \Phi_2) + \chi(1 - \Phi_2)^2 + V_2 \left(\frac{v_e}{V_0} \right) \left[(1 - \Phi_2)^{1/3} - \left(\frac{1 - \Phi_2}{2} \right) \right] \quad (6)$$

where a is the penetrant activity in the vapor phase, Φ_2 is the volume fraction of penetrant in the polymer, χ is the Flory–Huggins polymer–penetrant interaction parameter, V_2 is the penetrant molar volume, and v_e/V_0 is the cross-link density in the pure polymer (mol/cm³).

The maximum degree of cross-linking (v_e/V_0) in the polyimide is 3.9×10^{-4} mol/cm³, based on the available DABA units. Figure 8 shows the effect of cross-linking on CO₂ swelling in PDMS vs the experimental data of Fleming¹ where $v_e/V_0 = 1.24 \times 10^{-4}$. The effect of cross-linking is estimated from eq 6, where χ is a function of pressure⁵⁶ and $V_2 = 46$ cm³/mol, for values of swelling below 25%.¹ There is a negligible effect of cross-linking on the CO₂-induced swelling of PDMS, whereas the effect of cross-linking on swelling for the polyimides is very significant, as shown in Figure 4.

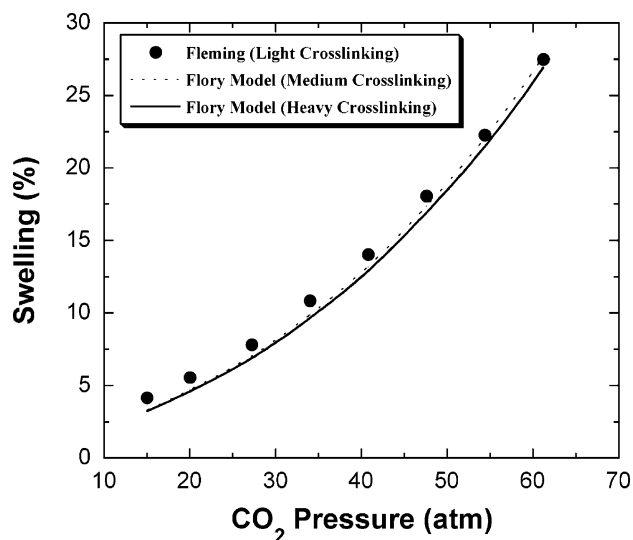


Figure 8. Effect of cross-linking on CO₂ dilation at various pressures with rubbery PDMS at 35 °C (cross-linking densities: $v_e/V_0 = 1.2 \times 10^{-4}$, 4.8×10^{-4} , and 1.4×10^{-3} mol/cm³).

High-pressure CO₂ permeation through lightly cross-linked PDMS has also shown plasticization effects.⁵⁷ However, the magnitude of this plasticization is fairly small and partially due to an upturn in the CO₂ sorption isotherm at ~ 27 atm at 35 °C. The pressure dependence of the permeability represents a balance between hydrostatic compressive forces that decrease free volume and plasticizing effects that increase free volume. Plasticization effects on the CO₂ permeability in glassy polymers are much greater because the diffusion coefficient is very sensitive to changes in the segmental mobility, whereas a rubbery polymer behaves more like a viscous liquid, which already has great mobility even in the absence of CO₂.

Conclusions

The CO₂-induced plasticization of 6FDA-DAM:DABA 2:1 polyimide films at 35 °C was characterized by comparing the swelling, sorption, and permeation responses to thermal annealing and covalent cross-linking. In situ spectroscopic ellipsometry is effective at simultaneously measuring the sorption and swelling in thin (~ 120 nm) polyimide films. Hysteresis in the swelling isotherm indicates that a glass transition was not induced by exposure to high-pressure CO₂ up to 80 atm.

Increased annealing temperatures resulted in better CO₂ permeation plasticization and organic solvent resistance for the films with free acid and cross-linkable ester groups. For the untreated membranes, the CO₂ permeability decreases with increased annealing temperatures. However, for the CHDM monoester, the CO₂ permeability increases as the polymer becomes more highly cross-linked, presumably due to chain-packing disruptions introduced by the cross-linking agents and the concomitant loss of bulky CHDM pendant groups in the cross-linking reaction. As the monoester becomes more highly cross-linked, sorption in the Henry's law mode decreases and sorption in the Langmuir mode increases, consistent with the free volume interpretation of the permeability data.

Increased annealing temperatures and chemical cross-linking of the polyimide films rigidifies the chains, which reduces the dilation of the polymer and, hence, controls the CO₂ diffusion coefficient. The local chain segmental

mobility appears to be reasonably correlated with the sorbed CO₂ partial molar volume, since the polymer swelling is normalized by the sorbed concentration. The plasticization pressure in permeation is approximately related to a threshold value of the sorbed CO₂ partial molar volume of $\sim 29 \pm 2$ cm³/mol in these polymers. These results suggest that plasticization (increases in the CO₂ diffusion coefficient) is caused by excessive polymer swelling, which can be controlled by rigidifying the polymer chains through annealing and cross-linking.

The thin films characterized with spectroscopic ellipsometry show lower CO₂ sorption than the bulk films measured by pressure-decay. There appears to be significantly greater physical aging for the thin films, as unrelaxed free volume elements are envisioned to leave the film by a diffusive mechanism. Ellipsometry enables the simultaneous measurement of swelling and sorption at length scales on the order of that of the permselective layers on asymmetric hollow fiber membranes. This technique can be used to probe thin polymer films under exposure to compressed fluids, which are beyond the resolution capabilities of more traditional dilation and sorption characterization techniques. Future work will focus on quantifying the effects of film thickness on plasticization with respect to sorption, diffusion, and swelling.

Acknowledgment. This research has been supported by United States Department of Energy Grant DE-FG03-95ER14538, National Science Foundation DMR-0072809, and the STC program of the National Science Foundation under Agreement CHE-9876674. The authors thank Joseph Pham for his help in preparing samples.

References and Notes

- (1) Fleming, G. K.; Koros, W. J. *Macromolecules* **1986**, *19*, 2285–2291.
- (2) Sefcik, M. D. *J. Polym. Sci., Part B: Polym. Phys.* **1986**, *24*, 935–956.
- (3) Wissinger, R. G.; Paulaitis, M. E. *J. Polym. Sci., Part B: Polym. Phys.* **1987**, *25*, 2497–2510.
- (4) Kamiya, Y.; Mizoguchi, K.; Terada, K.; Fujiwara, Y.; Wang, J. S. *Macromolecules* **1998**, *31*, 472–478.
- (5) Wessling, M.; Schoeman, S.; Boomgaard, T. v. d.; Smolders, C. A. *Gas Sep. Purif.* **1991**, *5*, 222–228.
- (6) Wessling, M.; Huisman, I.; Boomgaard, T. v. d.; Smolders, C. A. *J. Polym. Sci., Part B: Polym. Phys.* **1995**, *33*, 1371–1384.
- (7) Bos, A.; Punt, I. G. M.; Wessling, M.; Strathmann, H. *J. Membr. Sci.* **1999**, *155*, 67–78.
- (8) Sanders, E. S. *J. Membr. Sci.* **1988**, *37*, 63–80.
- (9) Goel, S. K.; Beckman, E. J. *AIChE J.* **1995**, *41*, 357–367.
- (10) Kazarian, S. G. *Appl. Spectrosc. Rev.* **1997**, *32*, 301–348.
- (11) Ohya, H.; Higashijima, T.; Tsuchiya, Y.; Tokunaga, H.; Negishi, Y. *J. Membr. Sci.* **1993**, *84*, 185–189.
- (12) Bos, A.; Punt, I. G. M.; Wessling, M.; Strathmann, H. *J. Polym. Sci., Part B: Polym. Phys.* **1998**, *36*, 1547–1556.
- (13) Staudt-Bickel, C.; Koros, W. J. *J. Membr. Sci.* **1999**, *155*, 145–154.
- (14) Wind, J. D.; Staudt-Bickel, C.; Paul, D. R.; Koros, W. J. *Ind. Eng. Chem. Res.* **2002**, *41*, 6139–6148.
- (15) Krol, J. J.; Boerrigter, M.; Koops, G. H. *J. Membr. Sci.* **2001**, *184*, 275–286.
- (16) Bos, A.; Punt, I. G. M.; Wessling, M.; Strathmann, H. *Sep. Purif. Technol.* **1998**, *14*, 27–39.
- (17) De Angelis, M. G.; Merkel, T. C.; Bondar, V. I.; Freeman, B. D.; Doghieri, F.; Sarti, G. C. *Macromolecules* **2002**, *35*, 1276–1288.
- (18) Sirard, S. M.; Green, P. F.; Johnston, K. P. *J. Phys. Chem. B* **2001**, *105*, 766–772.
- (19) Wessling, M.; Lopez, M. L.; Strathmann, H. *Sep. Purif. Technol.* **2001**, *24*, 223–233.
- (20) Torres, J. A.; Nealey, P. F.; de Pablo, J. J. *Phys. Rev. Lett.* **2000**, *85*, 3221–3224.
- (21) Forrest, J. A.; Dalnoki-Veress, K. *Adv. Colloid Interface Sci.* **2001**, *94*, 167–196.
- (22) Fleming, G. K.; Koros, W. J. *J. Polym. Sci., Part B: Polym. Phys.* **1987**, *25*, 2033–2038.
- (23) Sirard, S. M.; Ziegler, K. J.; Sanchez, I. C.; Green, P. F.; Johnston, K. P. *Macromolecules* **2002**, *35*, 1928–1935.
- (24) Wind, J. D.; Sirard, S. M.; Paul, D. R.; Green, P. F.; Johnston, K. P.; Koros, W. J. *Macromolecules* **2003**, *36*, 6442.
- (25) Husk, G. R.; Cassidy, P. E.; Gebert, K. L. *Macromolecules* **1988**, *21*, 1234–1238.
- (26) Wind, J. D.; Staudt-Bickel, C.; Paul, D. R.; Koros, W. J. *Macromolecules* **2003**, *36*, 1882–1888.
- (27) O'Brien, K. C.; Koros, W. J.; Barbari, T. A.; Sanders, E. S. *J. Membr. Sci.* **1986**, *29*, 229–238.
- (28) Koros, W. J.; Paul, D. R. *J. Polym. Sci., Part B: Polym. Phys.* **1976**, *14*, 1903–1907.
- (29) Cras, J. J.; Rowe-Taitt, C. A.; Nivens, D. A.; Ligler, F. S. *Biosens. Bioelectron.* **1999**, *14*, 683–688.
- (30) Azzam, R. M. A.; Bashara, N. M. *Ellipsometry and Polarized Light*; North-Holland Publishing Co.: Elsevier, 1977.
- (31) Tompkins, H. G.; McGahan, W. A. *Spectroscopic Ellipsometry and Reflectometry*; John Wiley & Sons: New York, 1999.
- (32) Obriot, J.; Ge, J.; Bose, T. K.; St-Arnaud, J. M. *Fluid Phase Equilib.* **1993**, *86*, 315–350.
- (33) Philipp, H. R. In *Handbook of Optical Constants of Solids*; Palik, E. D., Ed.; Harcourt Brace Jovanovich: Orlando, 1985; Vol. 1, p 749.
- (34) Jellison, G. E. *Opt. Mater.* **1992**, *1*, 41.
- (35) Zhou, H.; Liu, J.; Qian, Z.; Zhang, S.; Yang, S. *J. Polym. Sci., Part A: Polym. Chem.* **2001**, *39*, 2404–2413.
- (36) Wind, J. D. Ph.D. Dissertation, The University of Texas at Austin, 2002.
- (37) Salley, J. M.; Frank, C. W.; Miwa, T.; Roginski, R. *Adv. Polyimide Sci. Technol., Proc. Int. Conf. Polyimides, 4th* **1993**, 441–450.
- (38) Doolittle, A. K. *J. Appl. Phys.* **1951**, *22*, 1471–1475.
- (39) Cohen, M. H.; Turnbull, D. *J. Chem. Phys.* **1959**, *31*, 1164–1169.
- (40) Michaels, A. S.; Vieth, W. R.; Barrie, J. A. *J. Appl. Phys.* **1963**, *34*, 1–13.
- (41) McCaig, M. S.; Paul, D. R.; Barlow, J. W. *Polymer* **2000**, *41*, 639–648.
- (42) Vrentas, J. S.; Vrentas, C. M. *Macromolecules* **1991**, *24*, 2404–2412.
- (43) Wissinger, R. G.; Paulaitis, M. E. *Ind. Eng. Chem. Res.* **1991**, *30*, 842–851.
- (44) Fleming, G. K.; Koros, W. J. *J. Polym. Sci., Part B: Polym. Phys.* **1990**, *28*, 1137–1152.
- (45) Condo, P. D.; Johnston, K. P. *Macromolecules* **1992**, *25*, 6730–6732.
- (46) Kazarian, S. G.; Vincent, M. F.; Bright, F. V.; Liotta, C. L.; Eckert, C. A. *J. Am. Chem. Soc.* **1996**, *118*, 1729–1736.
- (47) Bolton, B. A.; Kint, S.; Bailey, G. F.; Scherer, J. R. *J. Phys. Chem.* **1986**, *90*, 1207–1211.
- (48) Lewis, J. E.; Biswas, R.; Robinson, A. G.; Maroncelli, M. *J. Phys. Chem. B* **2001**, *105*, 3306–3318.
- (49) Hayes, R. A. U.S. Patent 4,912,917, E. I. Du Pont de Nemours and Co.
- (50) Salley, J. M.; Frank, C. W. In *Polyimides: Fundamentals and Applications*; Ghosh, M. K., Mittal, K. L., Eds.; Marcel Dekker: New York, 1996.
- (51) Pitzer, K. S.; Brewer, L. *Thermodynamics (Revision of Lewis and Randall)*, 2nd ed.; McGraw-Hill: New York, 1961.
- (52) Struk, L. G. F. *J. Polym. Sci., Part B: Polym. Phys.* **1990**, *28*, 127–131.
- (53) Bohning, M.; Springer, J. *Polymer* **1998**, *39*, 5183–5195.
- (54) Eisenberg, A.; Hird, B.; Moore, R. B. *Macromolecules* **1990**, *23*, 4098–4107.
- (55) Flory, P. J. *Principles of Polymer Chemistry*, 15th ed.; Cornell University Press: Ithaca, NY, 1992.
- (56) Shim, J. J.; Johnston, K. P. *AIChE J.* **1989**, *35*, 1097–1106.
- (57) Jordan, S. M.; Koros, W. J. *J. Polym. Sci., Part B: Polym. Phys.* **1990**, *28*, 795–809.